

GYPSUM WEDGING AND CAVERN BREAKDOWN: STUDIES IN THE MAMMOTH CAVE SYSTEM, KENTUCKY

WILLIAM B. WHITE AND ELIZABETH L. WHITE

Materials Research Institute and Environmental Resources Research Institute, The Pennsylvania State University, University Park, PA 16802 USA

Many segments of dry passages in the Mammoth Cave System contain an unusual breakdown lying unconformably over underlying stream sediments. The association of many of these breakdown areas with sulfate minerals (primarily gypsum) suggests that crystal wedging and replacement of limestone by gypsum are important factors in this type of cavern collapse. The following features are characteristic of mineral-activated breakdown: 1) Walls and ceilings fractured in irregular patterns often with visible veins of gypsum following the fractures; 2) Breakdown consisting of characteristic thin, irregular splinters and shards of bedrock; 3) Curved plates of bedrock ranging in size from a few centimeters to more than a meter hanging from the ceiling at steep angles and cemented only by a thin layer of gypsum; 4) Collapses that take the form of symmetrical mounds with coarse irregular blocks at the base grading upward into a rock flour at the top. Thin sections of the curved plates clearly show gypsum replacing limestone. Possible sources for the sulfate-bearing solutions are from the weathering of pyrite either at the top of the overlying Big Clifty Sandstone or in the limestone wall rock surrounding the cave passage. Reactions of the percolating solutions produce sulfate minerals in the wallrock adjacent to cave passages. Gypsum and other sulfate minerals created in the wall rock are less dense than calcite and exert sufficient pressure to spall off bits of the rock, some of which remain cemented in place by the gypsum.

Breakdown occurs widely in caves. For the most part, breakdown results from simple mechanical processes of bed failure under gravitational load. Proposed failure mechanisms include brittle fracture of incompetent beams (White & White 1969, 2000) and failure by inelastic creep (Tharp 1994, 1995). Breakdown in dry caves generally requires some sort of initiation process such as the invasion of surface waters to widen fractures in otherwise stable rock layers. Existing breakdown piles can be removed by dissolution thus removing support from walls and ceilings and triggering new breakdown. Dissolution by vadose water moving along fractures can convert fixed beams into cantilever beams. These and related processes are well recognized and discussed in textbooks (e.g., Bögli 1980; White 1988; Ford & Williams 1989). The size and shape of breakdown fragments depends in a complicated way on preexisting conditions of bed thickness, the existence of partings along bedding planes, and density of fracturing that cuts across bedding as well as the shape of dissolution surfaces that exist prior to bedrock failure. The complexity of accurately classifying breakdown is discussed in some detail by Jameson (1991). The present paper concerns a special category of breakdown in which the initiating process is chemical reaction and wedging due to crystal growth rather than purely mechanical fracturing under gravitational load.

Piles of angular rock fragments near cave entrances formed by water freezing in fractures are observed in many caves. A layer of angular rock fragments in the sedimentary deposits in alpine caves has been ascribed to frost action deep in the bedrock during Pleistocene ice advances (Schmid 1958). In some caves, typically in very dry passages, there occurs breakdown composed of irregular fragments, shards and splinters

ranging in size from millimeters to a meter in width and fractions of a millimeter to a few centimeters in thickness. This breakdown is associated with gypsum deposition and was ascribed to crystal wedging effects (White & White 1969). Gypsum crystal wedging breakdown also has been described in the Friars Hole Cave System in West Virginia (Jameson 1991). Crystal wedging and spallation by the crystallization of halite has been described in the Nullarbor Caves in Australia (Lowry & Jennings 1974).

Crystal wedging breakdown and associated features are particularly well displayed in Turner Avenue in the Flint Ridge section of the Mammoth Cave System. Although the unusual breakdown in Turner Avenue has been recognized since the early exploration of the Flint Ridge Cave System (Smith 1964), no formal description of these deposits has been published. The objectives of the present paper are to describe in some detail the characteristic features of the gypsum wedging breakdown in Turner Avenue and to examine the geochemical mechanisms responsible for this particular breakdown process.

GEOLOGIC SETTING

Mammoth Cave is developed in the Mississippian St. Louis, Ste. Genevieve, and Girkin Limestones. Below the St. Louis is the relatively non-karstic Salem/Warsaw Formation, which acts as an aquiclude at the base of the section. Above the Girkin is the Big Clifty Sandstone which forms a protective caprock for the Mammoth Cave Plateau. The monoclinical structure dips to the northwest and is accompanied by minor folds and small-displacement faults. Details of the geology may be found in White et al. (1970), Palmer (1981), and White and

White (1989).

The great length of Mammoth Cave, ~570 km at the time of this writing, is possible because of interconnected groundwater basins with large surface catchment areas combined with survival of older passages protected by the overlying caprock. The time sequence represented by Mammoth Cave extends from the late Tertiary to the present (Palmer 2000; Granger *et al.* 2001). Upper level passages protected by the caprock tend to be dry. Passages that extend beneath the valley walls or that lie below valley floors tend to be wet. Growth of sulfate minerals and the process of crystal wedging take place in the very dry passages.

CHARACTERISTIC FEATURES OF CRYSTAL WEDGING BREAKDOWN

BREAKDOWN MORPHOLOGY

Evidence for crystal wedging can be found in many of the dry passages of Mammoth Cave, for example in Cleaveland Avenue, one of the main tourist routes. Similar evidence has been noted in other dry, gypsum-containing caves. The most extensive and best developed displays of crystal wedging breakdown occur in Turner Avenue, and for this reason, this area is described in some detail as the prototype to establish the diagnostic features of crystal wedging breakdown.

Turner Avenue extends from Argo Junction, a collapse on the wall of Houchins Valley, 2.9 km northward beneath Flint Ridge to another blockage at Brucker Breakdown (Brucker & Burns 1964). The north end is quite wet from vadose seepage and from vertical shafts, but the central portion of the passage, deep beneath the caprock on Flint Ridge, is extremely dry. Turner Avenue is an elliptical tube where not modified by breakdown. There is a shallow floor channel visible in many places. Scalloping near the floor of the conduit suggests final flow velocities of 10s cm/s. There is a thin layer of sand and silt sediment on the floor of the passage. Also in the sediment are some quartz pebbles from the basal conglomerate of the Pennsylvanian Caseyville Formation, which is exposed on Flint Ridge as a Pennsylvanian infilling of a late Mississippian paleochannel. The passage is at an elevation of 167 m and falls within Palmer's (1981) C level of Mammoth Cave. According to Granger *et al.* (2001), the quartz pebbles were deposited 1.46 Ma ago.

Breakdown deposits in Turner and Upper Turner Avenues often consist of masses of irregular slabs and other fragments that lie unconformably above the clastic sediments (Fig. 1). The breakdown is admixed with substantial amounts of gypsum. Gypsum forms along bedding planes and spreads over the passage walls as crusts (Fig. 2). Rubble piles of the sort shown in Figure 1 are suggestive but not diagnostic. More diagnostic of crystal wedging breakdown are the thin slabs that have apparently been split from the limestone beds. These grade downward into thin shards and splinters only millimeters thick (Figs. 3, 4). Crystal wedging breakdown is a subset of what Davies (1949) called "chip breakdown". Chip breakdown consists of rock fragments that are smaller than individual bedding



Figure 1. Rubble wall caused by gypsum deposition along bedding planes. Note hardhat for scale.



Figure 2. Wall of Turner Avenue showing extrusion of gypsum along bedding planes.

plane slabs and can result from many processes including purely mechanical ones.



Figure 3. Thin plates and other fragments, some held to the ceiling by gypsum, in Upper Turner Avenue (Type II breakdown). Hardhat provides scale.

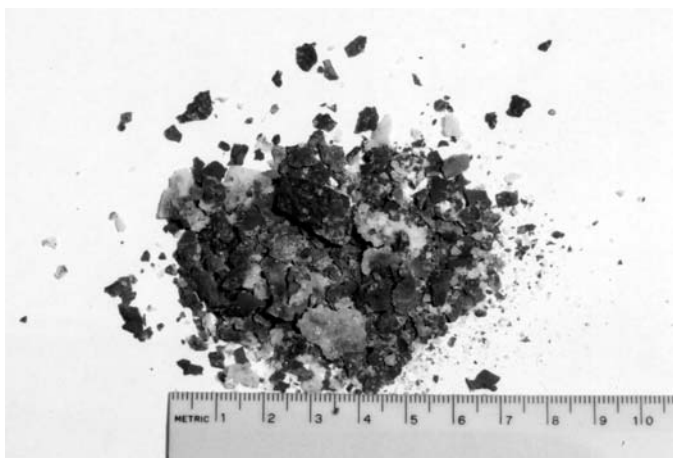


Figure 4. Breakdown splinters. Smallest rock fragments produced by gypsum-induced spalling.

Crystal wedging breakdown itself appears to be of two types. Type I consists of angular rock fragments broken on sharp planes that cut the bedding planes (Fig. 5). In the example shown, the fractures are filled with gypsum. Type I breakdown results from mechanical wedging due to crystallization of the gypsum. Similar rock fragments are found near cave entrances where they result from frost action. Type I crystal wedging breakdown results from purely mechanical pressures generated by crystal growing in small cracks and fractures. As an end member type, no chemistry is involved. Type II breakdown is more complex. The fragments and plates are angular,



Figure 5. Massive bedrock shattered by growth of gypsum in fractures producing Type I breakdown. Brunton compass provides scale.

sharp and are fractured across the usual zones of weakness – bedding planes and joints—as shown in Figures 3 and 4. Within this mass of fragments are small shards and splinters, only a few centimeters on a side and often less than a millimeter thick, which crush like broken glass when walked upon. These irregular plates, shards, and splinters are the signature of the crystal wedging process. The limestone bedrock is shattered and intermixed with gypsum so that entire passage walls become piles of rubble.

The thin shards of breakdown are also found in the ceilings completely surrounded by gypsum. It appears that they have been plucked from the bedrock ceiling and have remained embedded in the gypsum growth. At the northern end of Turner Avenue, where the passage becomes wet because of recent erosion of the caprock, some rock shards are found but the gypsum has been dissolved away.

CURVED BREAKDOWN PLATES

A less common but more diagnostic feature of gypsum wedged breakdown is shown in Figure 6. These are curved plates of limestone that appear to have been peeled from the ceiling and bent under their own weight. Some of these sagging beds take on a blister shape that appears to have been punched out of the ceiling (Fig. 6A). Close examination shows that these are indeed beds of limestone ~5 cm thick that are curved as though they had become plastic. Microscope examination of thin sections of the bent beds shows that the sagging and bending are due to the direct replacement of limestone by gypsum (Fig. 7A, B). Thin veinlets of gypsum occur throughout the solid slab of limestone. A total of 21 thin sections were prepared from breakdown slabs of various lithologies including some with no obvious curvature. Gypsum veinlets appear in most of them including the ones without obvious curvature.

The thin section data provide clear evidence that gypsum is not only crystallizing in joints and bedding plane partings, thus fracturing the rock, it is also crystallizing by direct chemical replacement of the limestone. Intrusion of gypsum causes the

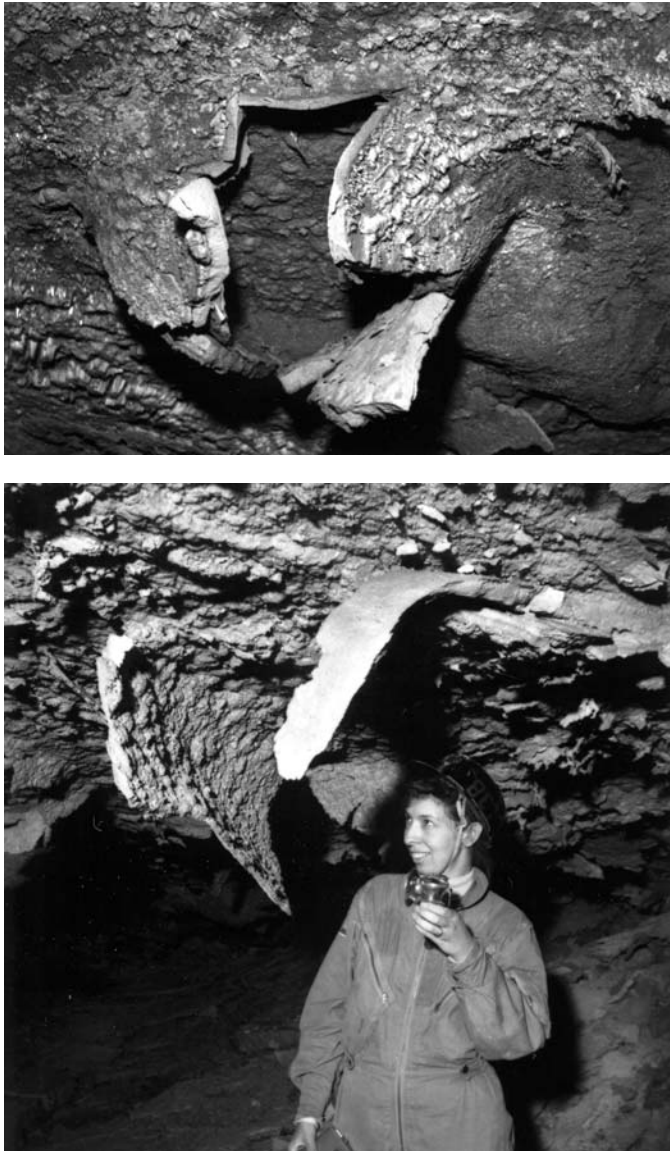


Figure 6. Curved breakdown slabs in Turner Avenue. (A-top) “Punch-out” of sagging bedrock slab. (B-bottom) Large curved plates.

limestone beds to swell and curve with the harder and more brittle limestone sliding along the softer gypsum. There are thus two processes, one mechanical and one chemical, acting together to produce Type II gypsum wedged breakdown.

MASSIVE COLLAPSE AND ROCK FLOUR

Additional evidence for the chemical intrusion of gypsum is provided by ruptured ceiling beds. Along Upper Turner Avenue, a sequence of rubble piles occur directly below collapse features in the ceiling (Fig. 8). The ceiling at the location shown in Figure 8 is a massive limestone bed 20–30 cm thick. Above the massive bed is a layer of thin-bedded limestone that has been extensively infused with gypsum. The gypsum formed in the thin-bedded limestone apparently built up sufficient pressure to force the collapse of the underlying massive

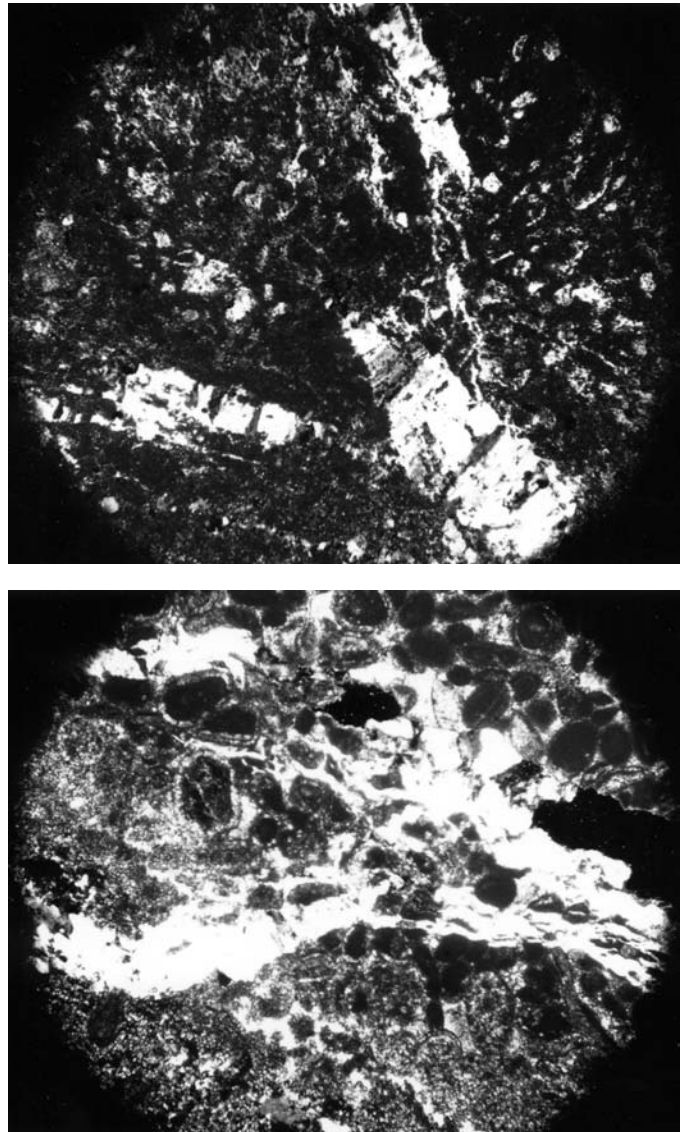


Figure 7. (A-top) Thin section of curved breakdown plate. Fine-grained material is limestone; large clear crystals are gypsum. (B-bottom) Thin section of curved breakdown plate showing limestone almost completely replaced by gypsum.

bed thus creating a collapse dome in the ceiling of the passage (Fig. 9). The debris pile is a chaotic mixture of rock fragments, gypsum crystals, and rock flour. The fragments of limestone appear to be etched and have very corroded surfaces.

Rock flour is characteristic of many of the gypsum wedged breakdown areas. Samples were collected from 5 locations and examined by x-ray diffraction, optical microscopy, scanning electron microscopy (SEM), and energy dispersive x-ray spectroscopy (EDX). The rock flour by microscope and x-ray evidence is found to be calcite dust mixed with ooids and fossil fragments. A minor amount of gypsum occurs in the rock flour. Scanning electron microscope images of rock flour sample 402 (Fig. 10A) reveals a uniform powder of strongly etched calcite

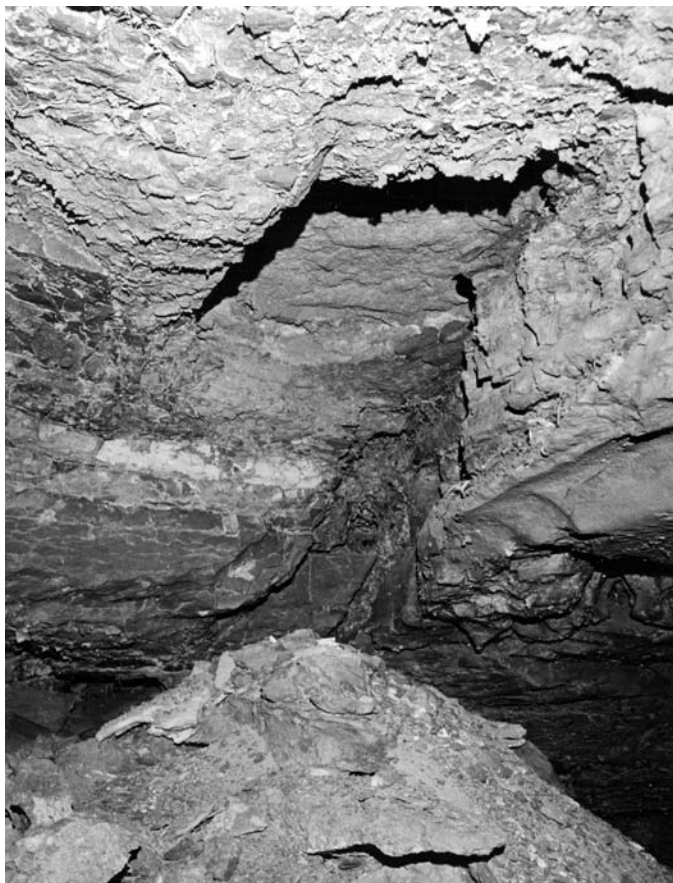


Figure 8. A ceiling breakout forming a rubble pile of rock fragments and rock flour.

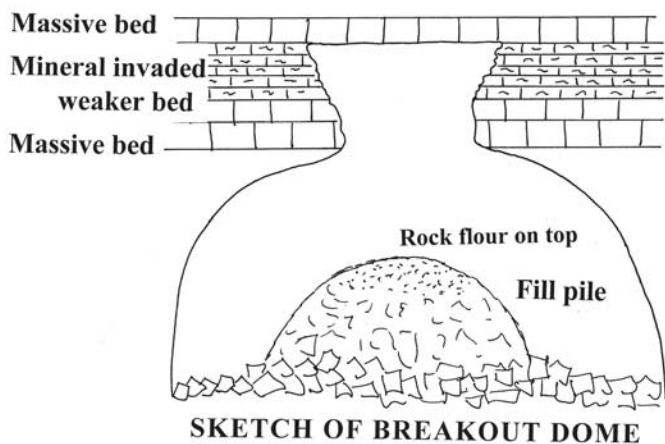


Figure 9. Sketch showing stratigraphic relations of ceiling breakout.

rhombs. Particle sizes are in the range of 10-50 μm . EDX analysis shows that some of the irregular small particles consist mainly of silica, presumably quartz. The SEM image of sample 408 (Fig. 10B) shows a more complex mixture. There are irregular rock fragments, some as large as one mm, mixed

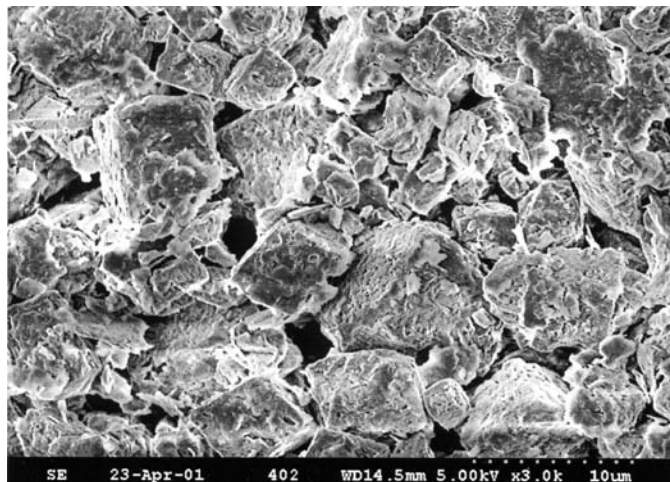


Figure 10. Scanning electron microscope images of rock flour. (A-top) Sample 402 from Turner Avenue consists mainly of etched calcite rhombs. (B-bottom) Sample 408 from Turner Avenue at intersection of Dead Bat Trail is a mix of limestone rock fragments (large lump), acicular gypsum crystals, and some minor quartz sand grains.

with irregular smaller particles and acicular crystals. EDX analysis shows the larger particles to contain mainly calcium with no other elements. This identifies them as calcite because carbon and oxygen do not appear in the EDX spectra. The absence of a magnesium peak suggests that the parent rock is limestone, not dolomite. Some of the smaller particles contain mainly silica, which is probably quartz. The acicular crystals contain both calcium and sulfur, thus identifying them as gypsum. A total of 30 images were obtained from various samples

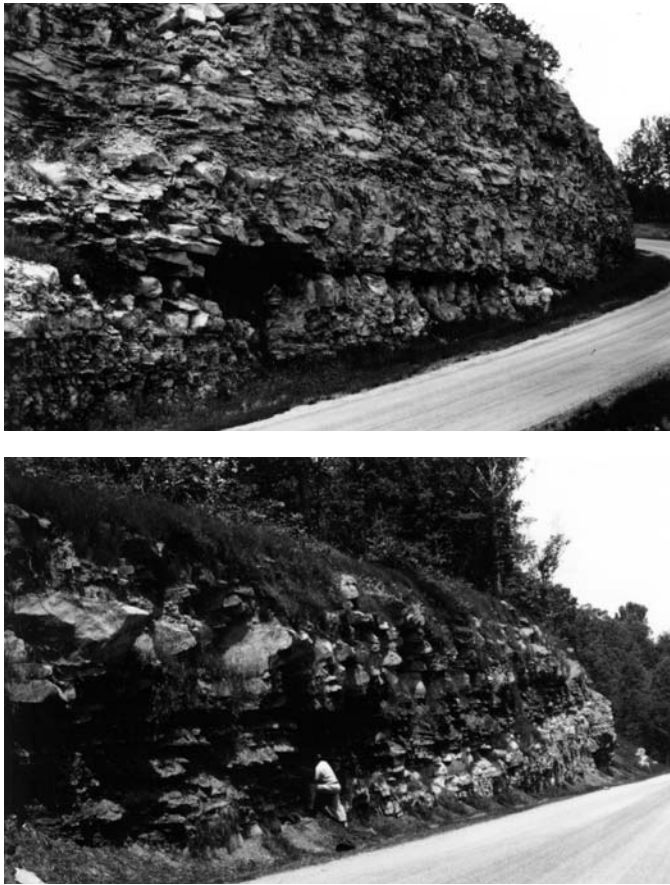


Figure 11. The contact between the Girkin Limestone and the Big Clifty Sandstone. (A-top) The road cut along Highway 70 on Joppa Ridge just west of the trail leading to Sandhouse Cave and Turnhole Spring. The contact is unconformable with the sandstone resting directly on the limestone. (B-bottom) Roadcut on Highway 422 near the Cedar Sink parking area. About 2 m of black impermeable shale separate the sandstone and the limestone. The separation of roadcuts (A) and (B) is 1.5 km.

taken at the 5 rock flour locations. The images were all variants on the two images reproduced in Figure 10. The rock flour appears to be residual debris from the chemical breakdown of the limestone bedrock.

BREAKDOWN MECHANISMS

GYPSUM SOURCES

Three hypotheses have been proposed to account for the gypsum in the caves of the Mammoth Cave region:

(1) Sedimentary anhydrite occurs in thin beds scattered through the Mississippian limestones, particularly the St. Louis Limestone. This anhydrite can be dissolved in circulating groundwater, transported to the caves, and redeposited as gypsum through evaporation (George 1977);

(2) Oxidation of pyrite that occurs disseminated, particu-

larly in the Girkin Limestone, provides sulfuric acid that reacts with the limestone to produce gypsum. Palmer (1986) and Palmer and Palmer (1995) proposed this source as part of their mechanism of gypsum deposition. Pyrite oxidation from a local source becomes part of what will be called the “Palmer Hypothesis”;

(3) E.R. Pohl long ago argued that the primary source of gypsum was oxidation of pyrite from a pyrite-rich layer at the top of the Big Clifty Sandstone (Pohl & Born 1935; Pohl & White 1965). This source will be incorporated in what will be called the “Pohl Hypothesis”.

The few measurements on sulfur isotope ratios that have been made seem to rule against sedimentary anhydrite as a primary source (Furman et al. 1999). Three samples of Mammoth Cave gypsum were analyzed giving $\delta^{34}\text{S}$ values of -5.06, -8.12, and -7.82, all in reasonable agreement with the values of -9 to -4.2 found for Mississippian pyrites but not in agreement with the values of -19 to -14 found for St. Louis anhydrites. This bit of evidence supports the hypothesis that the gypsum is derived from the oxidation of pyrite, not from the anhydrite that occurs interbedded in the limestones.

Pyrite does occur disseminated in the Girkin Limestone. Pyrite in the form of faceted crystals up to several millimeters in size has been observed by the authors. Palmer and Palmer (1995) have claimed, based on thin section evidence, that 0.1% of the rock mass is comprised of pyrite. They further claim that areas of extensive gypsum deposition coincide with areas of high pyrite concentration. According to the Palmer Hypothesis, the oxidation of pyrite, the reaction of sulfuric acid with the limestone to form gypsum, and the replacement of calcite by gypsum all take place in a relatively thin reaction zone surrounding the cave passage. No long distance transport mechanism is necessary.

Likewise, pyrite does indeed exist at the top of the Big Clifty Sandstone. Good exposures of this pyrite were directly visible in fresh roadcuts on Cane Run just north of the National Park that were made during the construction of the Nolin River Reservoir in 1963. The pyrite was associated with a coal-like organic layer and occurred in large quantities as nodules on the order of 10 cm thick. The organic bed was ~0.6 m thick and was estimated to contain 5-10% pyrite. X-ray diffraction of pyrite collected at this time confirmed the identification of the mineral. This deposit of pyrite was extremely reactive and oxidized very rapidly. Samples collected in the field were found to decompose in a few months even in sealed containers in the laboratory. Sulfuric acid was liberated and unidentified white fibrous crystals grew from the surface of the nodules. The pyrite disappeared very rapidly from exposed outcrops.

If the extensive pyrite at the top of the Big Clifty Sandstone is the source of the sulfate, rather than the sparse pyrite that occurs disseminated through the Girkin Limestone, there must be pathways for the migration of solutions through the sandstone and into the limestone. These pathways could also account for the spotty occurrence of sulfate minerals in the cave. Some dry areas contain a great deal of gypsum. Other dry

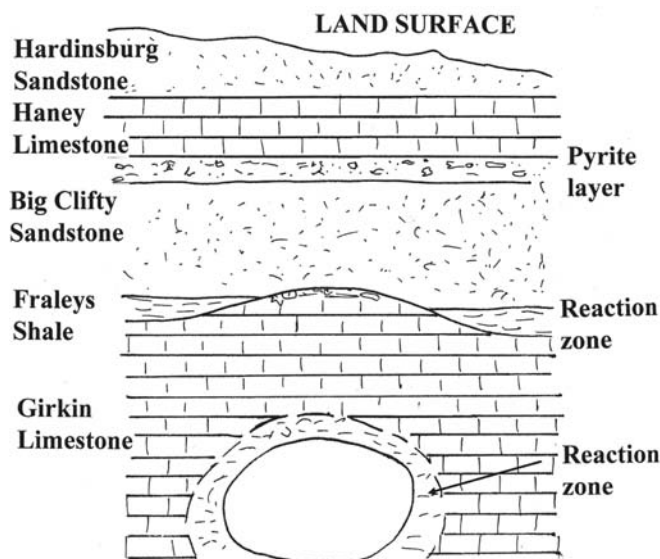


Figure 12. Sketch showing the physical model for transport of sulfate minerals from overlying Big Clifty Sandstone into cave passages in the limestones below.

areas are almost barren. The responsible geologic feature may be the Fraileys Shale. The Fraileys Shale is an intermittent black shale at the contact between the Big Clifty Sandstone and the Girkin Limestone. Where the shale is absent, the solutions can percolate down into the limestone. Where present, the shale presents a barrier and in these regions the underlying caves would be barren of gypsum. Figure 11 shows the Big Clifty/Girkin contact at 2 locations on Joppa Ridge, immediately south of Mammoth Cave Ridge. These photographs were taken in 1963 when the re-routing of Kentucky Route 70 produced fresh roadcuts. In one contact, the Big Clifty rests unconformably on the Girkin Limestone with no barrier to vertical percolation. In the other contact, less than a kilometer from the first, 2 m of black shale separate the 2 formations. At the time of this writing, the outcrop with the unconformable contact remains well exposed but weathering of the shale and growth of vegetation has largely concealed the other contact.

The oxidation of pyrite provides a source of sulfate ions and hydrogen ions. The iron released from the pyrite is not mobile and remains at the original location. Gypsum in the cave is generally free of iron-containing minerals. The sulfuric acid bearing solutions percolate very slowly through the Big Clifty and into the Girkin Limestone. Evidence from the breakdown, the breakout domes, and the rock flour suggests that the gypsum is formed *in situ* by chemical replacement of calcite in the wallrock immediately adjacent to the cave passages. Gypsum forms in a reaction zone in the cave passage walls regardless of the location of the pyrite.

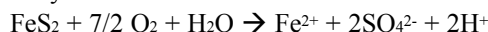
The physical model is sketched in Figure 12. The transport medium is the vertical percolation of groundwater in the vadose zone. There is a source area for sulfate ions and acidity at the top of the Big Clifty Sandstone. There are 2 reaction

zones, one at the contact between the sandstone and the Girkin Limestone and one in the wallrock immediately surrounding the cave passage.

CHEMISTRY OF PYRITE OXIDATION

Establishment of the chemical mechanism for gypsum deposition must be largely deductive because the slowly seeping solutions cannot be sampled. There is no liquid water in evidence in the gypsum areas. New growth over scratch marks and over areas where early Americans mined the sulfate minerals shows that the reactions must be proceeding under present-day conditions. The continued growth of gypsum and other sulfate minerals requires that slowly percolating solutions must exist in the pores and along fractures and bedding plane partings in the wallrock, although their chemistry remains unknown.

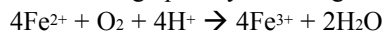
The chemistry of pyrite weathering has been extensively investigated because of its importance in understanding acid mine drainage (Langmuir 1997; Drever 1997). Pyrite is oxidized by the reaction



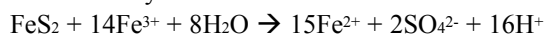
which produces for each mole of pyrite a mole of ferrous iron and two moles of hydrogen ion. The ferrous iron can oxidize slowly by a purely inorganic process to ferric iron which then precipitates as highly insoluble $\text{Fe}(\text{OH})_3$



thus releasing more acidity. Superimposed on these inorganic processes in mine spoil piles is an autocatalytic set of reactions mediated in large part by microorganisms.



The ferric iron then reacts with more pyrite to produce additional acidity.

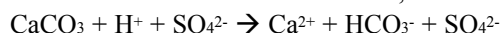


Although the detailed reaction mechanisms of pyrite oxidation either within the limestone bedrock or in the Big Clifty Sandstone are not known, the end products are the release of hydrogen ions and sulfate ions, which can ultimately react with calcite from the limestone to form gypsum.

GYPNUM DEPOSITION: THE POHL HYPOTHESIS

The physical model (Fig. 12) shows 2 possible reaction zones. One is at the contact of the Big Clifty Sandstone and the Girkin Limestone and the other is in the wallrock immediately surrounding the cave passage. Given a flux of sulfuric acid migrating downward from the Big Clifty, the task is to explain why the acidity is not completely neutralized at the limestone contact. It also is necessary to account for the evidence that gypsum is formed *in-situ* by replacement of calcite in the cave walls.

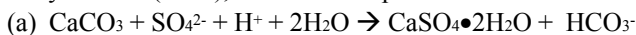
In an open system with continuously migrating solutions across the sandstone/limestone interface, the reaction would be



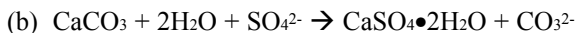
The reaction is written with sulfate ion on both sides of the equation to indicate that in this system, the sulfate ion is simply carried along in solution. All product ions would migrate

downward into the limestone dissolved in the vadose seepage. Because gypsum is ~10x more soluble than calcite, the ions remain in solution until the concentration builds up to gypsum saturation. This would take place on the cave walls because of evaporation of the solution. The bicarbonate ion would also be lost as CO₂ discharged into the cave atmosphere. In this system there might be breakdown due to crystal wedging because of crystallization of gypsum in fractures and bedding plane partings, but it is not clear whether or not there would be actual replacement of calcite by gypsum in the cave walls. One might see Type I breakdown but not Type II breakdown.

The reaction by which calcite is replaced by gypsum can be written in a number of ways. Two possible reactions, both noted by Palmer (1986), maintain all species in solution

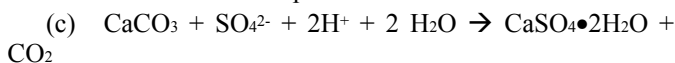


$$\frac{a_{\text{HCO}_3^-}}{a_{\text{H}^+} a_{\text{SO}_4^{2-}}} = K_a = 2.812 \times 10^6 = 10^{6.449}$$



$$\frac{a_{\text{CO}_3^{2-}}}{a_{\text{SO}_4^{2-}}} = K_b = 1.349 \times 10^{-4} = 10^{-3.870}$$

A third way is to assume that the reaction releases CO₂ gas. This should be appropriate for reactions in the walls of dry cave passages where all solutions eventually evaporate. There is transport of material into the cave by slow percolation of solutions in the vadose zone but there is no transport of material out of the cave. The replacement reaction can be written



$$\frac{P_{\text{CO}_2}}{a_{\text{H}^+}^2 a_{\text{SO}_4^{2-}}} = K_c = 1.914 \times 10^{14} = 10^{14.282}$$

where the a's are the activities of the designated ions. Numerical values for the equilibrium constants were calculated using Gibbs free energies of formation at 25° C from Drever (1997).

These reactions are not independent. All three are connected by the equilibria among the carbonate species. As a result $K_b/K_a = K_2$ and $K_a/K_c = K_1 K_{\text{CO}_2}$

Where K₁ and K₂ are the first and second ionization constants of carbonic acid and K_{CO₂} is the Henry's law constant for dissolution of gaseous CO₂ in water. Numerical values are given in Langmuir (1997) and Drever (1997).

The sulfate ion activity in the percolating solutions in the source area is unknown. It depends on the flux of slowly percolating solutions balanced against the weathering rate of pyrite deep within the bedrock. However, evaporation of the solutions in the vicinity of the cave passage must eventually

bring the solutions to saturation with gypsum if gypsum is to be deposited. At saturation,

$$a_{\text{Ca}^{2+}} a_{\text{SO}_4^{2-}} = K_{\text{gyp}} = 2.488 \times 10^{-5}$$

The solubility product constant for gypsum, K_{gyp}, at 25° C was calculated from Drever's (1997) thermodynamic data. Gypsum has a retrograde solubility but recalculating to 12° C only changes the solubility product constant to 2.510 x 10⁻⁵. The sulfate ion activity will be 4.958 x 10⁻³ for a solution saturated with gypsum. Inserting this into replacement equation (c) reduces it to

$$\text{Log } P_{\text{CO}_2} = 11.980 - 2\text{pH}$$

for limestone and gypsum coexisting in equilibrium.

Reaction of sulfuric acid with calcite at the Big Clifty/Girkin contact will release carbon dioxide into the pore spaces within the rock. When the CO₂ pressure exceeds atmospheric pressure, the CO₂ will be forced out of the reaction zone. According to the equation above, this will occur until the pH reaches 5.99. Thus much of the neutralization of acidity from the pyrite takes place in the reaction zone at the sandstone/limestone contact, generating Ca²⁺ ions and sulfate ions which are carried downward by vadose seepage. However, some residual acidity remains and can be carried downward into the limestone and the underlying cave passages. According to measurements by Miotke (1974), the CO₂ pressure in Mammoth Cave is exceptionally low, 10^{-3.3}, only a little above the outside atmospheric pressure, 10^{-3.47}. Continued replacement of calcite by gypsum in the wallrock with release of CO₂ into the cave atmosphere would proceed until the pH reaches 7.64 at which point the pressure of released CO₂ becomes equal to the CO₂ pressure of the cave atmosphere.

GYPSUM DEPOSITION: THE PALMER HYPOTHESIS

The Palmer hypothesis also depends on a flux of vadose seepage water originating at the land surface but with a different geochemical interpretation. Most limestone soils have CO₂ pressures in the range of 10⁻² to 10⁻¹ atm (1-10% CO₂ by volume). The soil water migrates downward to the limestone bedrock contact where it reacts, dissolving calcite to concentrations close to equilibrium at the P_{CO₂} of the soil. The water, with its dissolved load of Ca²⁺ and HCO₃⁻ ions, continues downward through pores and fractures in the bedrock until it reaches a cave passage where the CO₂ pressure is much lower, typically 10^{-2.5}. Excess CO₂ is degassed into the cave passage with concurrent precipitation of CaCO₃. This is the standard and long accepted mechanism for the deposition of calcite speleothems. Palmer (1986) notes that this mechanism assumes that the system is open so that the CO₂ consumed by dissolution of limestone at the soil/bedrock interface is replaced by fresh CO₂ from the overlying soil. The CO₂ pressure remains constant. He argues that vadose seepage waters in the sandstone-capped ridges of the Mammoth Cave area will behave as a closed system. The porous, sandy soils of the Mammoth Cave Plateau have typical CO₂ pressures of 10⁻³ to

$10^{-2.3}$ atm, only $\sim 10\times$ the CO_2 pressures in the cave atmosphere. When vadose water seeps through the sandstone to the underlying limestone, the dissolution reaction will proceed with CO_2 being consumed until the system comes to equilibrium.

Using a typical soil CO_2 concentration of 0.3% by volume ($P_{\text{CO}_2} = 10^{-2.5}$ atm), Palmer (1986) calculates a closed system P_{CO_2} of 4.5×10^{-5} atm ($10^{-4.35}$) and a pH of 8.85 for the seepage water when it reaches equilibrium. The calculated P_{CO_2} is not only lower than that of the cave atmosphere, it is lower than that of the surface atmosphere. A rough calculation using Langmuir's (1971) closed system model gives values of $P_{\text{CO}_2} = 10^{-4.12}$ and pH = 8.76 for an initial CO_2 concentration of 0.3 volume percent, which would be considered good agreement with Palmer's results.

The low CO_2 pressure in the seepage water emerging from the cave wall means that this water will absorb CO_2 from the atmosphere, become undersaturated, and can attack the limestone in the cave wall. Palmer uses this mechanism to account for the zones of active attack observed on cave walls including a location near Brucker Breakdown at the north end of Turner Avenue. Palmer's proposed mechanism accounts very nicely for the patches of "wet rot" observed at various places in the cave system. An additional question is whether or not the exceptionally low CO_2 pressure is sufficient to drive a direct replacement reaction of carbonate by sulfate.

Palmer uses reaction (b) to describe the carbonate replacement reaction. In order for this reaction to proceed to the right, it is necessary that the activity ratio

$$\frac{a_{\text{SO}_4^{2-}}}{a_{\text{CO}_3^{2-}}} \geq \frac{1}{K_b}$$

It may be assumed that the pore fluids are saturated with gypsum and thus the sulfate ion activity is determined by the solubility constant for gypsum. The carbonate ion is a minor species in the pH range of 8-9. The carbonate ion activity can be calculated from the estimated CO_2 pressure of the pore fluids in terms the various carbonate equilibrium constants and the pH.

$$a_{\text{CO}_3^{2-}} = \frac{K_1 K_2 K_{\text{CO}_2} P_{\text{CO}_2}}{a_{\text{H}^+}^2}$$

If we take the sulfate ion activity = 4.958×10^{-3} and choose CO_2 pressures of 4×10^{-4} atm, the cave atmosphere and 4.5×10^{-5} according to Palmer's (1986) calculation for the closed system pore fluid, the sulfate/carbonate activity ratio is 48 and 352 respectively. The calculations outlined in the previous section give $1/K_b = 7400$. Palmer (1986) gives 5400 and Palmer and Palmer (1995) give 4900. For the estimated pore fluid chemistry, the sulfate/carbonate activity ratio is about an order of magnitude short of what is needed to drive the direct replacement reaction. In order to drive the direct replacement reaction, the closed system needs to pull down the CO_2 pres-

sure of the vadose seepage solutions by at least another order of magnitude. Whether or not this may actually happen is difficult to determine in the absence of any chemical data on the pore fluids.

COMPARISON OF HYPOTHESES

It is emphasized that the oxidation of pyrite will produce acidity which can react directly with limestone to produce Ca^{2+} and SO_4^{2-} . These ions will combine to form gypsum where ever the solutions are allowed to evaporate. Gypsum can be formed from the oxidation of pyrite in the limestone and it can form from vadose seepage carrying ions from the pyrite zone at the top of the Big Clifty. Either hypothesis can provide the gypsum but both hypotheses have difficulty explaining the direct observational evidence that calcite replacement by gypsum takes place in the cave walls.

The Palmer hypothesis is the most direct in that all reactions take place immediately in the site of gypsum deposition and formation of the gypsum crystal breakdown. It requires that the highly irregular distribution of gypsum in the cave be dictated by the distribution of pyrite in the limestone. There is a question of whether the volume of pyrite is sufficient to account for the large volumes of gypsum observed in the cave. If this gypsum is indeed derived from pyrite in the adjacent wall rock, it is curious that there is so little iron hydroxide in evidence.

The Pohl hypothesis has the advantage that very large masses of pyrite are available at the top of the Big Clifty Sandstone. Iron compounds resulting from the oxidation of the pyrite would remain in the upper Big Clifty, conveniently out of sight. The distribution of gypsum would be controlled by the distribution of the Fraileys Shale, also an unknown quantity. The difficulty is in maintaining a chemical driving force for the replacement of calcite by gypsum in the cave walls.

It should also be noted that these hypotheses are not mutually exclusive. Both sources may be functional, including the possibility that one may dominate in some locations in the cave while the other source may dominate in other locations.

CRYSTAL WEDGING

The chemical reaction that describes the replacement of calcite by gypsum shows that the replacement takes place on a mole-for-mole basis. Decomposition of one mole of calcite produces one mole of gypsum. The replacement, however, results in a volume expansion of about a factor of two. Using the calcite unit cell parameters of Reeder (1983) with 2 formula units of CaCO_3 per unit cell gives a molar volume of 61.305 \AA^3 whereas the unit cell parameters for gypsum (Cole & Lancucki 1974) with 4 formula units per unit cell give a molar volume of 123.59 \AA^3 . It is this large volume expansion that is responsible for the mechanical wedging that produces the fracturing of the shards and splinters as well as the curved breakdown plates.

Palmer and Palmer (2000) have calculated a somewhat different mechanism for replacement of calcite by gypsum in the

sulfuric acid caves such as Carlsbad and Lechuguilla. Their mechanism involves a reaction in which 2 moles of calcite are replaced by one mole of gypsum with the other half of the calcium being carried off in solution. With this mechanism, there would be an almost negligible volume expansion because of the fortuitous approximately 1:2 ratio in the molar volumes of calcite and gypsum. The replacement reactions in sulfuric acid caves differ from those in the dry passages of Mammoth Cave in that the reactions were assumed to take place when the caves were water-filled. In Mammoth Cave, all water is lost by evaporation and the mechanism would not apply.

CONCLUSIONS

Examination of the breakdown in many sections of Mammoth Cave but particularly in Turner and Upper Turner Avenues in the Flint Ridge Section of the cave reveals evidence for crystal wedging and chemical replacement by gypsum and other sulfate minerals as the primary mechanism for the breakdown. Field evidence includes bedrock fractured into slabs, shards, and splinters of many sizes; breakdown consisting of curved rock slabs; breakout domes with a rubble of rock fragments; gypsum crystals; and rock flour. Laboratory evidence includes microscopic examination of thin sections that show calcite replacement by gypsum. X-ray powder diffraction, optical microscopy, scanning electron microscopy, and energy dispersive x-ray spectroscopy of the rock flour show it to be a reaction product of calcite replacement. The geochemistry of gypsum deposition is examined in some detail. Possible sources of gypsum include a pyrite-rich horizon at the top of the Big Clifty Sandstone and pyrite dispersed in the Girkin Limestone.

ACKNOWLEDGMENTS

The samples described in this paper were collected under permit from the National Park Service. We are grateful to the Superintendent and staff of Mammoth Cave National Park for their support of this work. The late E.R. Pohl provided many helpful discussions and also showed us the pyrite exposures at Nolin River Reservoir. We thank Maria Klimkiewicz for measuring the SEM images and A.N. Palmer for his comments on the geochemistry of sulfate deposition. This project was supported by the Cave Research Foundation.

REFERENCES

- Bögli, A., 1980, Karst hydrology and physical speleology: Springer-Verlag, Berlin, 284 p.
- Brucker, R.W., & Burns, D.P., 1964, The Flint Ridge Cave System: Cave Research Foundation, Yellow Springs, OH, Folio 3 p text + 31 maps.
- Cole, W.F., & Lancucki, C.J., 1974, A refinement of the crystal structure of gypsum $\text{CaSO}_4 \cdot 2\text{H}_2\text{O}$: *Acta Crystallographica*, v. B30, p. 921-929.
- Davies, W.E., 1949, Features of cavern breakdown: *National Speleological Society Bulletin*, v. 11, p. 34-35, 72.
- Drever, J.I., 1997, The geochemistry of natural waters: 3rd ed.: Prentice Hall, Upper Saddle River, NJ, 436 p.
- Ford, D.C., & Williams, P.W., 1989, Karst geomorphology and hydrology: Unwin-Hyman, London, 601 p.
- Furman, F.C., Gregg, J.M., Palmer, A.N., & Shelton, K.L., 1999, Sulfur isotopes of gypsum speleothems in the central Kentucky karst system: Indications of pyrite and anhydrite sulfur sources, and sulfuric acid karstification: *MSM Spelunker*, v. 42, n. 1, p. 20-24.
- George, A.I., 1977, Evaluation of sulfate water quality in the north-central Kentucky karst, in Dilamarter, R.C., & Csallany, S.C., (eds.) Hydrologic problems in karst regions: Western Kentucky University, Bowling Green, KY, p. 340-356.
- Granger, D.E., Fabel, D., & Palmer, A.N., 2001, Pliocene–Pleistocene incision of the Green River, Kentucky, determined from radioactive decay of cosmogenic ^{26}Al and ^{10}Be in Mammoth Cave sediments: *Geological Society of America Bulletin*, v. 113, p. 825-836.
- Jameson, R.A., 1991, Concept and classification of cave breakdown: An analysis of patterns of collapse in Friars Hole Cave System, West Virginia, in Kastning, E.H., & Kastning, K.M. (eds.), *Appalachian karst*: National Speleological Society, Huntsville, AL, p. 35-44.
- Langmuir, D., 1971, The geochemistry of some carbonate ground waters in central Pennsylvania: *Geochimica et Cosmochimica Acta*, v. 35, p. 1023-1048.
- Langmuir, D., 1997, *Aqueous Environmental Geochemistry*: Prentice Hall, Upper Saddle River, NJ, 600 p.
- Lowry, D.C., & Jennings, J.N., 1974, The Nullarbor karst Australia: *Zeitschrift für Geomorphologie*, v. 18, p. 35-81.
- Miotke, F.D., 1974, Carbon dioxide and the soil atmosphere: *Abhandlungen zur Karst-und Höhlenkunde*, v. A9, p. 1-49.
- Palmer, A.N., 1981, A geological guide to Mammoth Cave National Park: Zephyrus Press, Teaneck, NJ, 196 p.
- Palmer, A.N., 1986, Gypsum replacement of limestone by alternating open and closed systems in the vadose zone, Mammoth Cave, Kentucky: Cave Research Foundation Annual Report, p. 27-28.
- Palmer, A.N., & Palmer, M.V., 1995, Geochemistry of capillary seepage in Mammoth Cave: Proceedings of Mammoth Cave National Park's Fourth Science Conference, p. 119-133.
- Palmer, A.N., 2000, Speleogenesis of the Mammoth Cave System, Kentucky, U.S.A: Chap. 5.3.8, in Klimchouk, A., Ford, D.C., Palmer, A.N., & Dreybrodt, W (eds.), *Speleogenesis: Evolution of karst aquifers*: National Speleological Society, Huntsville, AL, p. 367-377.
- Palmer, A.N., & Palmer, M.V., 2000, Hydrochemical interpretation of cave patterns in the Guadalupe Mountains, New Mexico: *Journal of Cave and Karst Studies*, v. 62, p. 91-69.
- Pohl, E.R., & Born, K.M., 1935, Development of gypsum in limestone caves: Proceedings of the Geological Society of America, p. 96.
- Pohl, E.R., & White, W.B., 1965, Sulfate minerals: Their origin in the central Kentucky karst: *American Mineralogist*, v. 50, p. 1461-1465.
- Reeder, R.J., 1983, Crystal chemistry of the rhombohedral carbonates: *Reviews in Mineralogy*, v. 11, p. 1-47.
- Schmid, E., 1958, Höhlenforschung und Sedimentanalyse, *Schriften des Institutes für Ur- und Frühgeschichte*, v. 13, 186 p.
- Smith, P.M., 1964, The Flint Ridge Cave System: 1957-1962: *National Speleological Society Bulletin*, v. 26, p. 17-27.
- Tharp, T.M., & Holdrege, T.J., 1994, Fracture mechanics analysis of limestone cantilevers subjected to very long-term tensile stress in natural caves: Proceedings of the 1st North American Rock Mechanism Symposium, A.A. Balkema, Rotterdam, p. 817-824.
- Tharp, T.M., 1995, Design against collapse in karst caverns, in Beck, B.F., & Pearson, F. (eds.), *Karst geohazards*, A.A. Balkema, Rotterdam, p. 397-406.
- White, E.L., and White, W.B., 1969, Processes of cavern breakdown: *National Speleological Society Bulletin*, v. 31, p. 83-96.
- White, E.L., and White, W.B., 2000, Breakdown morphology: Chap. 6.2, in Klimchouk, A.B., Ford, D.C., Palmer, A.N., and Dreybrodt, W. (eds.), *Speleogenesis: Evolution of karst aquifers*: National Speleological Society, Huntsville, AL, p. 427-429
- White, W.B., 1988, *Geomorphology and hydrology of karst terrains*: Oxford University Press, New York, 464 p.
- White, W.B., Watson, R.A., Pohl, E.R., and Brucker, R., 1970, The central Kentucky karst: *Geographical Review*, v. 60, p. 88-115.
- White, W.B. and White, E.L., 1989, *Karst Hydrology: Concepts from the Mammoth Cave area*: Van Nostrand-Reinhold, New York, 346 p.